KSÜ Mühendislik Bilimleri Dergisi, 27(2), 2024
Araştırma Makalesi

KSU J Eng Sci, 27(2), 2024
Research Article

Kahramanmaras Sutcu Imam University
Journal of Engineering Sciences

Geliş Tarihi : 12.10.2023
Kabul Tarihi :11.11.2023

Received Date : 12.10.2023
Accepted Date : 11.11.2023

INVESTIGATION OF THE FRACTURE BEHAVIOR OF GEOPOLYMER CONCRETE REINFORCED WITH RECYCLED STEEL AND GLASS FIBERS

GERİ DÖNÜŞTÜRÜLMÜŞ ÇELİK LİF VE CAM ELYAFI KULLANILARAK GÜÇLENDİRİLMİŞ GEOPOLİMER BETONLARIN KIRILMA DAVRANIŞININ İNCELENMESİ

Hakan BAYRAK[1*] (ORCID: 0000-0001-9441-2214)
Muhammed GÜMÜŞ[1] (ORCID: 0000-0002-7380-0098)

[1] Kafkas Üniversitesi, İnşaat Mühendisliği Bölümü, Kars, Türkiye

*Sorumlu Yazar / Corresponding Author: Hakan BAYRAK, hbayrak@kafkas.edu.tr

ABSTRACT

The brittleness of the geopolymer composites is an issue for its widespread use worldwide. Therefore, several types of fibers have been added to the geopolymer mixture to provide a ductile manner. In this work, the recycled steel fibers were employed in a hybrid form with glass fibers to take advantage of the low carbon emission in the production process of recycled steel fibers. The total fiber content was taken as constant 0.6% by volume. Five dissimilar geopolymer batches were handled and two concrete prisms were cast for each batch. Those prisms were tested under three-point loading and the deformed shapes of the specimens' surface were captured by digital camera to generate the surface displacement field. The fracture characteristics of the notched prisms were criticized in terms of (i) load-CMOD response, (ii) crack progress ahead of the pre-notch, (iii) fracture energy, (iv) ultimate load-bearing capacity, and (v) unstable fracture toughness. Test results revealed that the residual strength, the ultimate load, and the fracture energy of fiber-reinforced geopolymers had a decreasing trend with the increasing recycled steel fiber ratio in the hybrid blend. The reasonable cause of that finding was the heterogeneous distribution of the recycled steel fibers.

Keywords: Geopolymer, recycled steel fiber, glass fiber, digital image correlation, notched prism

ÖZET

Geopolimer kompozitlerin gevrek davranışı, dünya çapında yaygın kullanımı için bir sorundur. Bu nedenle geopolimer karışımına süneklik sağlamak amacıyla çeşitli tiplerde lifler eklenmiştir. Bu çalışmada, geri dönüştürülmüş çelik liflerin üretim sürecindeki düşük karbon emisyonundan yararlanmak amacıyla, geri dönüştürülmüş çelik elyaflar cam elyaflarla birlikte hibrit formda kullanıldı. Toplam lif içeriği hacimce %0,6 sabit olarak alınmıştır. Beş farklı geopolimer karışımı hazırlanmış ve her karışım için iki beton prizma dökülmüştür. Bu prizmalar üç noktalı yükleme altında test edildi ve numunelerin yüzeyinin deforme şekli, yüzey yer değiştirme alanını oluşturmak için dijital kamera ile kaydedildi. Çentikli prizmaların kırılma özellikleri (i) yük-CMOD davranışı, (ii) çentik önündeki çatlak ilerlemesi, (iii) kırılma enerjisi, (iv) nihai yük taşıma kapasitesi ve (v) kararsız kırılma tokluğu açısından değerlendirildi. Test sonuçları, hibrit karışımdaki geri dönüştürülmüş çelik lif oranının artmasıyla birlikte lifli geopolimerlerin artık dayanımları, nihai yükü ve kırılma enerjisinin azalma eğiliminde olduğunu ortaya çıkardı. Bu durumun geri dönüştürülmüş çelik liflerin beton içerisindeki heterojen dağılımından kaynaklandığı düşünülmektedir.

Anahtar Kelimeler: Geopolimer, atık çelik lif, cam lifi, dijital görüntü korelasyonu, çentikli prizma

ToCite: BAYRAK, H., & GÜMÜŞ, M., (2024). INVESTIGATION OF THE FRACTURE BEHAVIOR OF GEOPOLYMER CONCRETE REINFORCED WITH RECYCLED STEEL AND GLASS FIBERS. *Kahramanmaraş Sütçü İmam Üniversitesi Mühendislik Bilimleri Dergisi*, 27(2), 386-400.

INTRODUCTION

Traditional concrete materials were regarded as indispensable construction materials due to their featured mechanical properties until a few decades ago. Ordinary Portland cement is used as a main traditional concrete material; however, the entire cement production process generates a large number of greenhouse gases and harmful emissions (Anvari & Toufigh, 2022), including carbon dioxide and sulfur dioxide (Farhan et al., 2018). Several studies have shown that one-ton cement production releases one-ton carbon dioxide, also total global carbon dioxide emissions released from cement production are approximately 5 – 7 % (Wang Z. et al., 2023; da Silva et al., 2022; Ren & Li, 2022; Wang Yijiang et al., 2020). Furthermore, cement production requires continuous electrical energy. Therefore, it causes very high levels of energy consumption (Zada Farhan et al., 2022). Due to the mentioned disadvantages, especially environmental ones, research has focused on the production of cement-free concrete materials by preserving the mechanical properties of concrete used in the construction sector (Laxmi & Patil, 2022). Eventually, studies indicate that geopolymer concrete manufacturing emits significantly less carbon dioxide than ordinary Portland cement concrete (Khan et al., 2022; Li et al., 2022). Additionally, the energy usage during the production of geopolymer concrete is significantly lower compared to ordinary Portland cement concrete with equivalent strength (Sherwani et al., 2022). In addition, it is revealed that the solidified state of the geopolymers displays superior mechanical and durability characteristics in comparison to those of ordinary cement-based concrete (Ding et al., 2016). Several investigations regarding geopolymer concretes focused on gathering fresh insights into the effect of mixture component ratios on the final material's strength, and physical and mechanical properties (Meskhi et al., 2023). For example, one study analyzed the impact of fly ash and waste glass powder (WGP) in specific ratios on geopolymer concrete (GPC) by varying the proportions of molarity and WGP percentage in GPC (Çelik et al., 2023). In addition, in some studies, waste or recycled materials were utilized to enhance the mechanical properties of geopolymers while considering environmental factors (Başaran et al., 2023; Özkılıç et al., 2023). Unfortunately, the brittleness of geopolymer concretes continues to be an issue due to their highly amorphous intrinsic structures. To address this problem, fibers were added to the mixtures in their fresh state (Davidovits, 1991). Since then, several types of fibers have been applied to improve the brittle characteristics of the geopolymer concretes (Laxmi & Patil, 2022; Ranjbar & Zhang, 2020). Recent research employs innovative ideas and technologies, including 3D printing of fiber-reinforced geopolymer concrete. Further studies must focus on the analysis of the properties of compositions acquired through various binder and activator types in order to advance this field (Meskhi et al., 2023).

Adding various types of fibers has become a widely utilized technique in engineering applications to overcome the disadvantages described earlier in geopolymer concrete (Wang T. et al., 2023). Generally, the fibrous materials utilized to enhance the performance of geopolymer concrete fall into two categories: industrial fibers and natural fibers (Vijaya Prasad et al., 2022). Industrial fibers can be classified into three main types: steel, synthetic, and inorganic. On the other hand, natural fibers are typically composed of animal, plant, and mineral fibers. Among all the fibers, steel fibers with varying geometric shapes were the most preferred type (Rashad, 2020). The primary rationales for selecting steel fibers are their cost effectiveness, high density, and high tensile strength (Pająk & Ponikiewski, 2013). In addition, studies have shown that the benefits of incorporating steel fibers can be summarized as follows (Aisheh et al., 2022; Vijaya Prasad et al., 2022): (i) improvement of ductility, toughness and flexural strength of geopolymer concrete (ii) improvement of impact and fatigue resistance of structural materials (iii) reducing the permeability, creep and shrinkage of polymer concrete (iv) increasing amount of absorbing energy. Despite these advantages, using industrial steel fibers in eco-friendly geopolymers would increase their carbon footprint. The production of just one ton of concrete and steel emits 0.9 and 1.9 tons of CO_2 into the atmosphere respectively (Isa et al., 2020). The result of another study shows the undesirable fact that industrial steel fibers account for 40% of the total carbon emissions of standard cement-based concrete containing 1.5% volume of fibers (Mastali et al., 2018). These problems have been partially addressed by utilizing recycled steel fiber in place of industrial steel fiber (Qin & Kaewunruen, 2022; Simalti & Singh, 2021). Due to this advantageous property of recycled steel fiber, recent research has focused on the incorporation of recycled steel fiber into geopolymer concrete. Several empirical researches have been carried out to uncover the impact of recycled steel fibers on the mechanical characteristics of geopolymer composites. One of the studies, conducted by (Yolcu et al., 2022), examined how the dose of binder affects the mechanical and durability properties of recycled steel fiber-reinforced geopolymers. According to findings, increasing the binder dosage enhances mechanical features such as compressive, flexural, and splitting tensile strength. In another study, researchers stated that recycled steel fibers may decrease the workability of fresh geopolymer mixtures. However, these fibers also have a favorable effect on the compressive and flexural strength of hardened geopolymer concrete (Eskandarinia et al., 2022).

In addition to the significant effect of recycled steel fiber, in certain studies, recycled steel fibers have been hybridized to capitalize on the synergistic impact of other fiber types. One study employed both industrial and recycled steel fibers to create a hybrid form. (Alsaif & Abdulrahman S. Albidah, 2022). The study demonstrated that the hybrid steel fibers address the reduction in strength of the geopolymer as a result of the waste tire rubber additives. Another conducted study (Zhong et al., 2019) examined the geopolymer concretes, which incorporate waste tire rubber and recycled steel fibers at different dosages. The results revealed that the addition of recycled steel fibers not only enhanced the flexural response after the peak load but also restored the reduced compressive strength caused by crumb rubber. In addition to the studies on hybridized geopolymer concrete, the research (Wang Yi et al., 2020) presents an experimental study examining the impact of hybrid polyvinyl alcohol and recycled tire steel fibers on the engineering properties of fly ash-slag-based strain-hardening geopolymer composites. The obtained results show that the strain-hardening geopolymer composite's resistance to drying shrinkage and compressive strength were improved significantly. Nonetheless, hybridizing polyvinyl alcohol fiber with recycled tire steel fiber caused a noteworthy reduction in flowability, setting time, and flexural strength of strain-hardening geopolymer composite. Eventually, studies have shown that recycled steel fibers can be combined with various fibers to improve the strength of geopolymer concrete. Additionally, fiber additives can improve the post-peak flexural response of quasi-brittle materials by bridging cohesive cracks. One highly effective additive for achieving this advantageous situation is glass fiber. The research (Kumar et al., 2022) indicates that the incorporation of glass fiber can prevent microcracks in geopolymer concrete. This study suggests that glass fiber may enhance the toughness of geopolymer concrete, resulting in a highly dense and crack-free geopolymer matrix with improved toughness. Another study (Rashedi et al., 2022) also demonstrated that the inclusion of glass fiber, an inorganic, non-metallic material, into geopolymer concrete offers great insulation, robust heat and corrosion resistance, and high mechanical strength. However, its drawbacks lie in brittleness and poor wear resistance. On the other hand, there is no existing study that explores the utilization of recycled steel fibers combined with glass fibers in geopolymer concrete, even though glass fibers offer favorable properties. Hence, it is evident that there is a need for a specific study in which the hybrid blend of glass and recycled steel fibers is investigated as the main parameters in terms of fracture characteristics of geopolymer composites.

In light of the literature review, the main distinctive feature of the present study is to blend the recycled steel and the glass fibers and to use this hybrid fiber form to improve the fracture characteristics of geopolymer concrete. The notched prism specimens were produced to evaluate the influence of blends obtained by hybridizing both fibers on the fracture behavior of geopolymer concrete. A total of ten prisms geopolymer concrete specimens with 100x100x400 mm were formed by pouring two specimens from each of 5 different mixes. All the specimens underwent testing using a deformation-controlled quasi-static three-point bending load. The cohesive crack's formation and propagation were documented using the two-dimensional digital image correlation technique. The test results were analyzed for (i) Load-CMOD responses, (ii) crack growth process, (iii) fracture energy, (iv) ultima load resisting capacity, and (v) unstable fracture toughness. Despite the limited number of samples, these findings can broaden our current understanding of the fracture behavior of a mixture of recycled steel and glass fiber-reinforced geopolymers.

EXPERIMENTAL PROGRAM

Material Properties

The geopolymer concrete samples produced in this study contain a total of 6 different ingredients: Slag, marble, sodium silicate, sodium hydroxide, recycled steel, and glass fiber. Ground granulated blast-furnace slag was utilized as the aluminosilicate source material in the blend. The manufacturer reported that the slag has a specific gravity of 2.9 g/cm^3 and a specific surface of 5445 cm^2/g. Marble powder used in the geopolymer concrete was intentionally selected as the filling material to mitigate environmental concerns. The marble powder exhibited a particle size range of 0 to 400 microns. In addition to the marble powder, no other coarse or fine aggregate has been used in the blend. A combination of sodium silicate and sodium hydroxide solution was used to activate the aluminosilicate precursor. The concentration ratios of the solutions were employed as 36% for the sodium silicate and 48% for the sodium hydroxide. The density of the sodium silicate and sodium hydroxide solutions was approximately 1.38 g/cm^3. Also, the molarity of the sodium hydroxide solution was 12 M. Another ingredient utilized in the concrete mixture was the recycled steel fibers having a peak frequency of about 10% in fiber length corresponding to the range of 24-28 mm. Another additive used in this study the glass fibers exhibit high resistance to both alkaline and acidic environments, rendering them suitable for use in highly alkaline geopolymer concrete without any adverse effects(Ganesh & Muthukannan, 2021). Several essential mechanical and physical properties of the glass fiber used in the compound

are as follows. Young's modulus and tensile strength of glass fiber are 72 GPa and 1700 MPa, respectively. A visual representation of the constituents used to manufacture the geopolymer composites is shown in Figure 1.

Notched Beams

In this study, it is aimed to examine fracture mode 1 for the produced specimens. To achieve this goal, it is necessary to determine the crack mount opening displacement of the beam under the applied load. Before testing the beams, a notch is made at the center of each beam. The peak point of the notch is then used as a reference to determine the crack mount opening displacement with the aid of 2D digital image correlation. Therefore, ten notched prism specimens were produced utilizing five different mix ratios. The substances utilized in the production of the geopolymer composites are displayed in Table 1. As shown in the table, notch prisms were named according to the proportions of the fiber content used in volume for the sample design. The letters in the name of the sample indicate the type of fiber used, while the numbers following them indicate the percentage by volume of that fiber in the sample. As illustrated in the table, the blend in the top row has no fiber, whereas all other blends contain at least one fiber type. Also, the fiber content in the blends with fiber is 0.6% of the total volume. For example, the mixture's name G0.4S0.2-I/II indicates that the blend contains 0.4% glass fiber and 0.2% recycled steel fiber by volume. Also, I/II demonstrates that identical two samples were generated from every mix ratio. As shown in the table, the ratio of precursor to activator (the sum of sodium silicate and sodium hydroxide) is equal to 2. In addition, the ratio of sodium silicate to sodium hydroxide was 2,5. For each mixture, those ratios were kept constant. However, to ensure the volume stability of the mixture, the quantity of marble powder was adjusted to range from 785-801 kg/m3.

Figure 1. A Sketch of Concrete Production Process

Table 1. The Mixture Compositions for The Geopolymer Concrete (kg/m^3)

Mix ID	Slag	Marble powder	Sodium silicate	Sodium hydroxide	Steel fiber	Glass fiber	Total mass (kg)
G0S0-I/II	1008	801	360	144	0	0	2313
G0.6S0-I/II	1008	785	360	144	0	15.5	2312.5
G0.4S0.2-I/II	1008	785	360	144	15.7	10.3	2323
G0.2S0.4-I/II	1008	785	360	144	31.3	5.2	2333.5
G0S0.6-I/II	1008	785	360	144	47	0	2344

To enhance the uniformity of the mixture, the slag and marble powder were initially dry-blended for one minute. Next, the solution of sodium silicate and sodium hydroxide was added to the dry mixture and continued blending for an additional four minutes. Then, recycled steel fibers were added to the fresh mixture to obtain steel fiber-reinforced concretes. Special care was taken to avoid fiber clumping when adding steel fibers. During the next minute of mixing, the fibers were slowly dispersed into the mixture. Next, the fresh mixtures were poured into the wooden molds which had a clear dimension of 100x100x400 mm3. To prevent evaporation, the open surfaces of the molds were covered with thin plastic films. Approximately 24 hours after casting, the specimens were taken out from their molds and submerged in a water tank for water curing until the day of testing. Before conducting the experiments, edge notches perpendicular to the longitudinal axis of the specimens were created by cutting them with a circular concrete saw. The depth of the notch remained constant, measuring 30 mm for every specimen, and all notches were drilled at the center of each specimen as shown in Figure 2. In the present study, the deformations on the sample surface were determined using 2D digital image correlation using the photos taken during the test. To achieve this goal, the specimens' surface was initially coated with white paint. Then, speckle patterns on the newly formed white background were created.

Test Configuration

The experimental setup utilized in this study is illustrated in Figure 2. As shown in the figure, the clear span length of the specimen was set to 300 mm, resulting in a span-to-depth ratio of 3. The notched beams were subjected to a bending load with controlled deformation. Throughout the experiment, the loading rate remained constant at 0.05 mm/minute for the plain specimens. For fiber-reinforced specimens, the loading rate was gradually increased until the specimen completely failed. At the stroke length of 0 to 1.5 mm, a loading rate of 0.3 mm per minute was applied. Then, the loading rate increased rapidly to 1.0 mm/minute and 2.0 mm/minute once the testing machine's stroke length surpassed 1.5 mm and 6.5 mm deflection, respectively. The load data was acquired from the load cell on the loading machine and recorded via computer software. The vertical and horizontal deformation maps of the sample surface were calculated from the series of deformed images. The experiment captured the distorted shapes of the specimen, which cannot be detected by the naked eye, within a 5-second interval. To capture those images, a Canon 6D Mark II digital camera and a Canon 50mm f/1.4 USM lens were utilized. Moreover, LED light sources were operated to enhance the contrast between the white background and the dots on it, as shown in Figure 2. In this study, the resolution of the image was approximately 14 pixels per millimeter. Some important DIC parameters used for the analysis of the images were the subset diameter, subset space, and strain radius, which were taken as 50, 20, and 5 pixels respectively. The images have been analyzed using an open-source algorithm (Blaber et al., 2015).

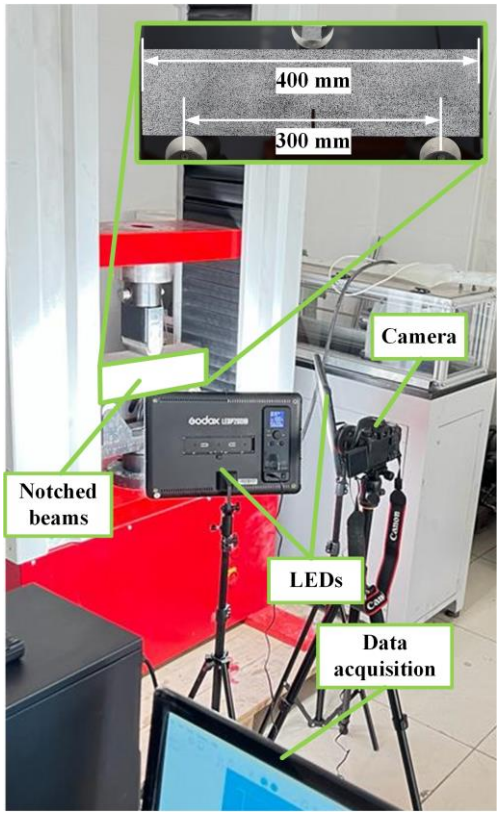

Figure 2. A Representative Review of The Bending Test Setup

RESULTS AND DISCUSSIONS

Load versus CMOD Curves

When quasi-brittle materials such as concrete are considered, crack mouth opening displacement (CMOD) is required for defining the material behavior. Figure 3 cooperatively illustrates experimental load versus CMOD curves. In the figure, the possible distribution regions were colored grey. As seen from the figure, the response curves of identical specimens were rather similar to each other. The relatively long tail of the specimen G0S0-II compared to the companion specimen may be attributed to the saw-tooth crack path and thereby the shear stress at the crack surfaces. The bending tests of the fiber-reinforced concrete were terminated at about 8 mm vertical deflection value, which corresponds to approximately 11 mm CMODs as in Figure 3.

Effects of the fiber inclusion were evident in the figure. In comparison with fiber-reinforced specimens, plain specimens had a rather low CMOD capacity which was smaller than 1.5 mm. Besides, the load-bearing capacity of the plain specimens was remarkably lower than that of the fiber-reinforced geopolymers. Those findings were not surprising. The distributed fibers help to stress transfer between the cohesive crack formed at the post-peak zone, which provides the specimens with an enhanced peak load and the ductility level. The other convenient result achieved from Figure 3 is about the rate of stress decay after the peak load is reached. When the ratio of the recycled steel fibers raised from 0 to 0.6% at an interval of 0.2%, the residual strength at the 4 mm of CMOD was recorded as 3.2 kN, 2.0 kN, 1.4 kN, and 0.77 kN, respectively. Accordingly, it can be noted that the glass fibers were a much more influential parameter on the deceleration of strength decay also increasing the ductility of geopolymer specimens.

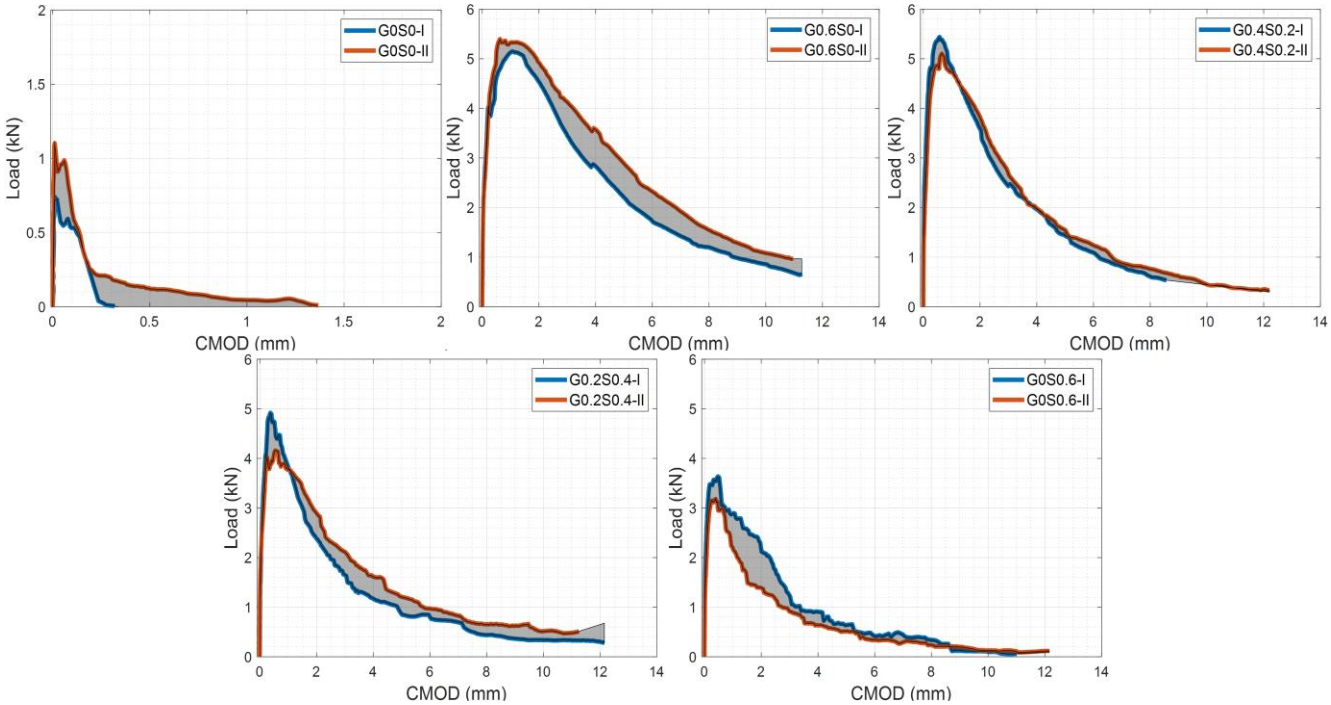

Figure 3. Load Versus Crack Mouth Opening Displacement Curves

Crack Progress

The crack trajectory of the specimens may serve as an indicator of the overall performance of the notched specimens. As shown in Figure 4, the representative cracking process for the plain specimen (G0S0-I), glass fiber reinforced specimen (G0.6S0-I), and recycled fiber reinforced specimen (G0S0.6-I) was displayed for the varying loading from 20% of the peak load to the peak load at an interval of 20%. Besides, an additional image was also given for the 80% of the peak load at the post-peak region.

It can be observed from Figure 4 that the initial cracking point can be distinguishable. For the G0S0-I, the cracking point was located between 40% and 60% of the peak load, whereas, for the G0.6S0-I and G0S0.6-I specimens, the initial cracks were formed before 20% of the peak load. In terms of the load magnitudes, the cracking loads corresponded to 0.14 kN, 0.99 kN, and 0.76 kN, respectively for the G0S0-I, G0.6S0-I, and G0S0.6-I specimens. Hence, it can be stated that the fiber inclusion significantly improved the cracking load capacity (approximately 607% for the glass fiber and 443% for the recycled steel fiber). Those increments in the cracking load capacity could be attributed to the fiber bridging effect on the cohesive zone.

The other finding is on the multiple crack distributions on the specimens' surface. At first, it should be noted here that the initial cracks were not visible by the naked eye, but only observable through the image analysis. After a while, the major cracks were accompanied by multiple minor cracks in the vicinity of the initial notches. Minor cracks simultaneously developed until the peak loads for the plain specimen of G0S0-I. In the case of fiber-reinforced members, they progressed up to 60% of the peak loads for G0.6S0-I and 80% of the peak loads for G0S0.6-I, respectively. Compared to the plain specimens, therefore, it may be deduced that the distributed fibers compelled the major crack to be localized long before the peak load. Such an experimental result was in good agreement with the literature (Gümüş & Arslan, 2019).

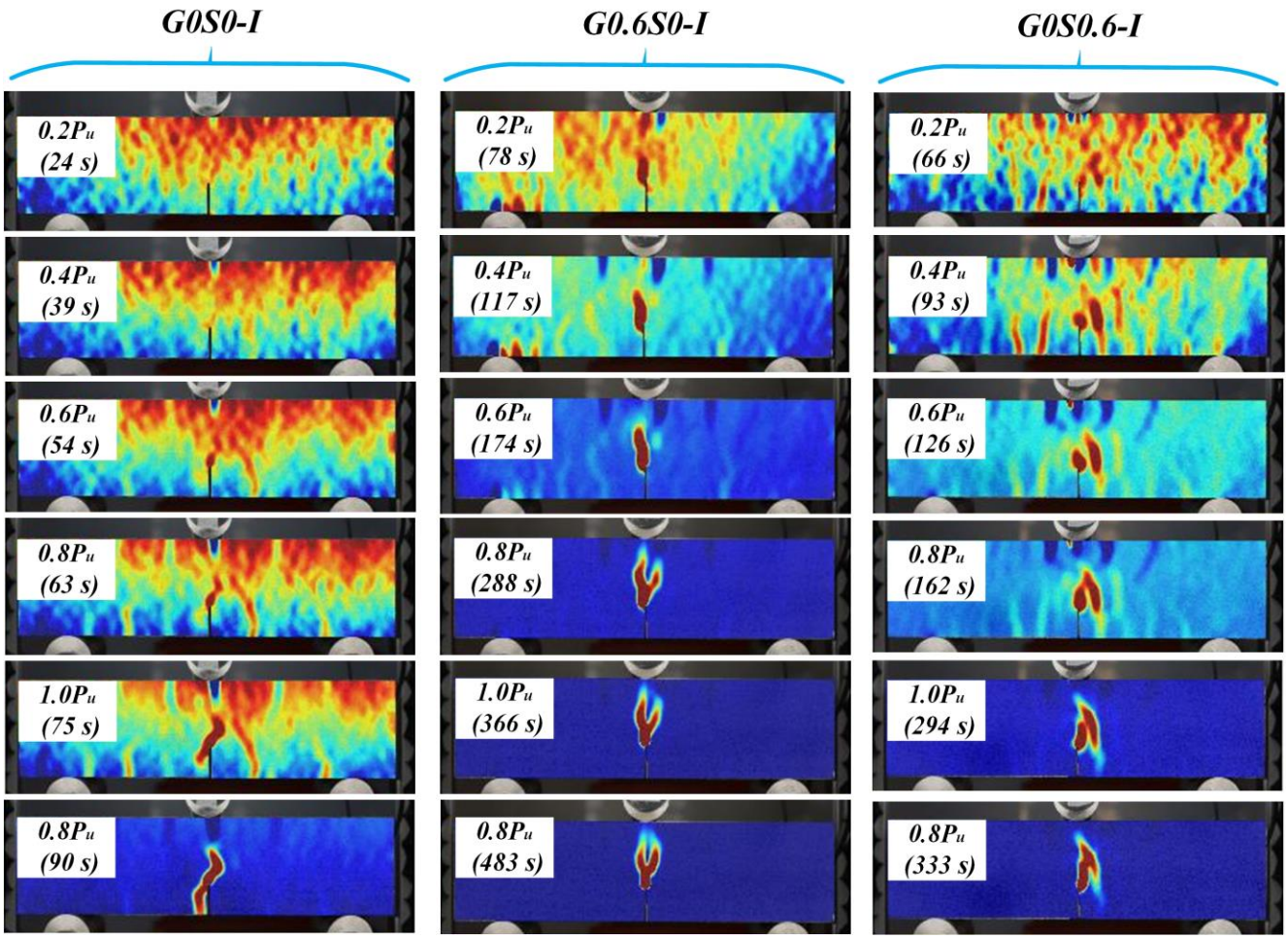

Figure 4. Crack Progress on The Surface of Some Selected Specimens

Fracture Energy

The fracture energy may be referred to as energy required for the failure of the specimens and is of significant fracture parameter for the fiber-reinforced concrete. Because the use of steel fibers mainly improves the post-peak residual strength of plain specimens, while a remarkable enhancement in the ultimate load capacity is obtained. That explanation could be noticeable in the experimental load-deflection curves in Figure 5. From the figure, the strength decay was significantly influenced by the existence of the fibers. The fracture energy used in this section was computed by the following equation (RILEM TCS, 1985).

$$G_F = \frac{W_0 + mg\delta_0}{b(h-a_0)} \tag{1}$$

In Eq. 1, the notation of W_0 symbolizes the area under the experimental load-deflection response in Figure 5. m and g are the mass between the support and the acceleration of gravity, while δ_0 represents the ultimate deflection in Figure 5. b, h, and a_0 point out the geometrical factors such as depth, width, and the notch length of the specimens.

Figure 6 designates the relation between the predicted fracture energies and the fiber content in the hybrid form. Accordingly, the use of the dispersed fibers increased the fracture energies of the plain specimen. The average fracture energy of 0.03 N/mm for the plain specimens reached 2.99 N/mm and 1.14 N/mm on average for G0.6S0 and G0S0.6 specimens, respectively. Then, it can be highlighted that the fraction of the recycled steel fibers in the hybrid form played a mitigating role in the fracture energy of the geopolymer concrete compared to the specimens in which glass fiber content was higher than the steel fiber. Such a result was much more evident when a comparison was made on the results of fiber-reinforced specimens. The mean fracture energy proportionally declined from 2.99 N/mm to 1.14 N/mm by increasing recycled steel fiber content from 0 to 0.6% by volume, which corresponded to a 61.9% drop in magnitudes. That unfavorable effect of recycled steel fibers may stem from the uneven distribution of the fibers. Standard deviations of the specimens given in Figure 6 support the irregular distribution of the fibers.

Besides, the other reason may be the bonding strength between the individual fibers and the surrounding matrix. The plastic remnant on the steel fibers could result in a weak bonding compared to that between the glass fibers and the matrix. Strength decay rate at the post-peak zone of fiber reinforced geopolymer also supports that statement. When the ratio of the recycled steel fiber in the hybrid form rose, not only peak strength but also residual strength at an arbitrary deflection level decreased as observed in Figure 5 due to the relatively low bonding strength of recycled fibers.

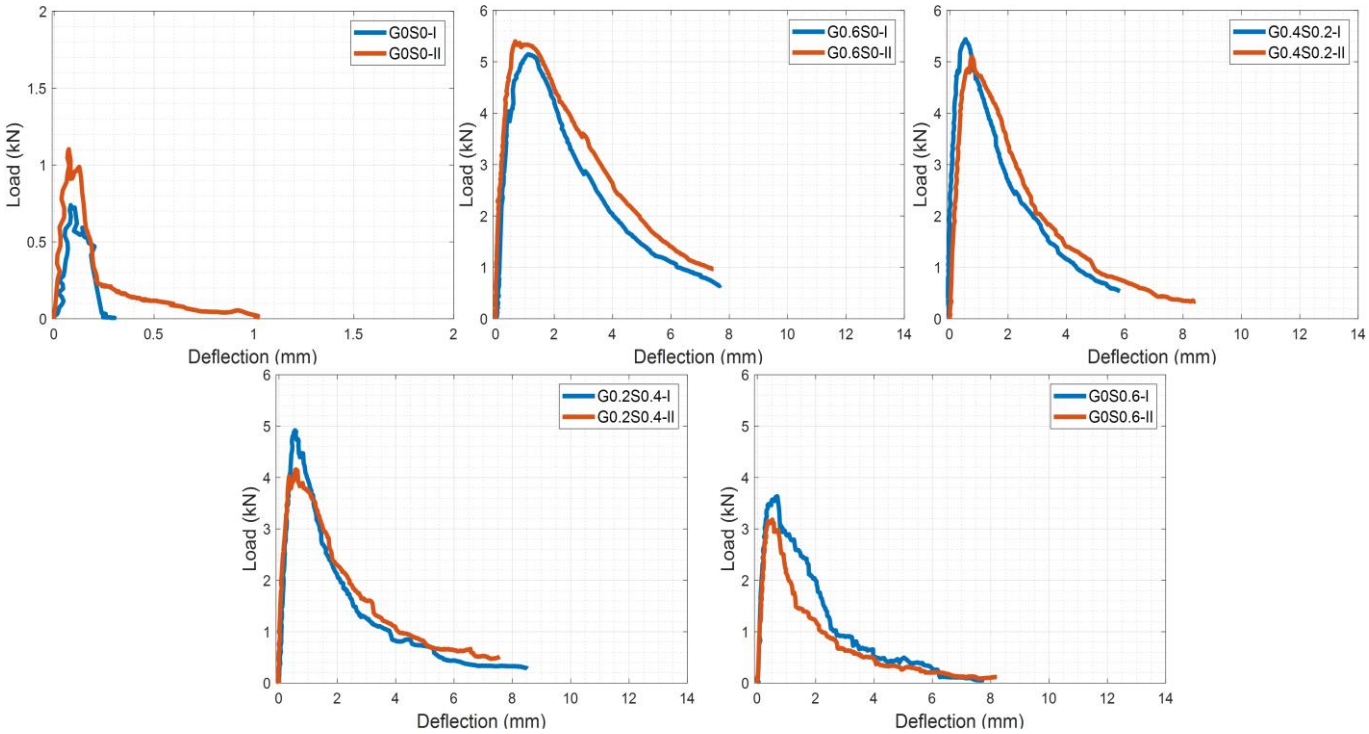

Figure 5. Experimental Load-Deflection Responses of The Notched Beams

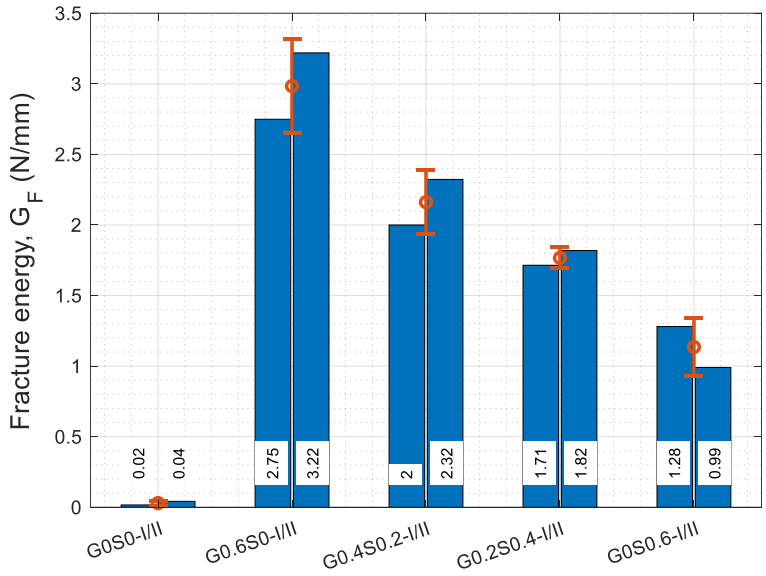

Figure 6. Variation and Standard Deviation of Fracture Energies with The Fiber Content in Hybrid Form

Ultimate Load Resisting Capacity

Figure 7 illustrates the distribution of the peak loads recorded during the experiments. In the figure, average magnitudes and the standard deviations are also presented. Compared to the peak loads of the fiber-reinforced specimens, plain specimens had significantly low load-resisting capacities. The use of the fibers caused a jump in the load capacity of the plain specimens by at least 2.7-fold in the case of the G0S0.6 mixture. This conclusion is caused by the bridging effect of the fibers. Mono fibers dispersed throughout the cohesive zone ahead of the initial notch

provide additional strength capacity by transferring the stresses between the crack faces. However, the magnitudes of the stresses conveyed between the crack faces rely on both fiber's properties and the bonding characteristics between the fibers and the corresponding matrix. That is why the ultimate load capacity of the fiber reinforced specimens was not identical as seen in Figure 7. Examining the volume fraction of recycled steel fibers, the peak load was first constant at 5.27 kN, when the steel fiber content changed from 0 to 0.2 vol%. Then, it gradually diminished as the steel fiber content was further increased. The specimens having the minimum peak loads were the G0S0.6-I/II such that the average load was 3.41 kN. Hence, a 35.3% reduction was acquired by replacing the glass fibers (G0.6S0) with recycled steel fibers (G0S0.6).

The other expressive conclusion is obtained by comparing Figure 6 and Figure 7 to evaluate which mechanism is most influenced by the fiber additives. At first glance, the overall shape of Figure 6 and Figure 7 seems to be similar. However, by comparing the increment ratio, it could be achieved that the fibers influenced the area under the load-deflection curves more than the peak load. For instance, when the glass fibers were used at 0.6 vol% ratio (G0.6S0), the average peak load and the fracture energy raised by 4.73-fold and 98.67-fold, respectively. Similarly, when the recycled steel fibers were used at 0.6 vol% ratio (G0S0.6), the peak load and the fracture energy increased by 2.71-fold and 37-fold, respectively. The other outcome is based on the effectiveness of the fiber type. As seen from the numbers given above, recycled steel fibers were less effective for both fracture energy and the peak resisting load capacity compared to glass fibers.

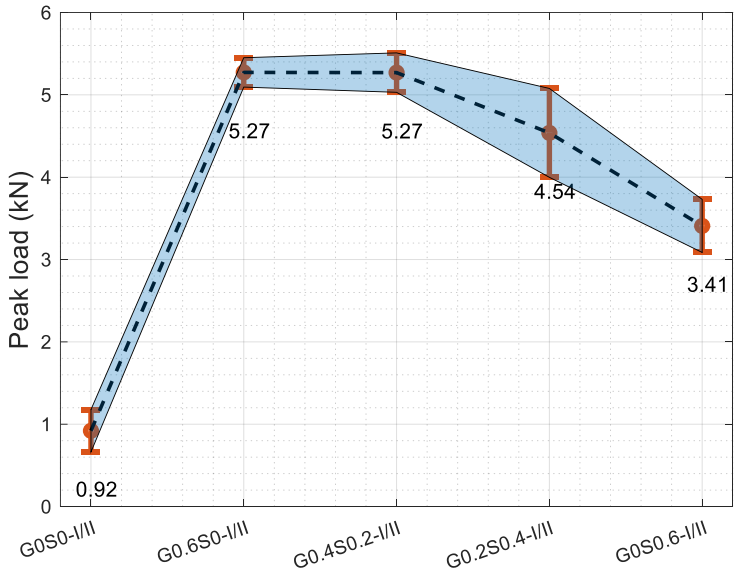

Figure 7. Peak Load Distribution of The Fiber-Reinforced Geopolymers

Unstable Fracture Toughness

Fracture toughness points out the resisting ability of a specimen having an existing defect against rapid crack growth. When the peak load and the corresponding crack length are considered, the fracture toughness is termed unstable fracture toughness. Although the crack length may be able to be predicted by using the analytical method (Jenq & Shah, 1985), in the present study, experimental crack length was evaluated in the calculation of unstable fracture toughness.

Figure 8 illustrates the cracking shapes as well as the crack lengths at the ultimate loading states. On average, the crack length of the plain specimens was 65.6 mm, which was the lowest one compared to that of the fiber-reinforced geopolymers. As the recycled steel fibers increased in the hybrid blend from 0 to 0.6%, the mean crack length continuously raised from 83.7 mm to 90.8 mm, which implied an increment of about 8.5%. The brittleness of the plain matrix is known to be higher in comparison with the fiber-reinforced concrete. Accordingly, the crack length of the plain specimens was expected to be higher than that of the fiber-reinforced specimens. However, the initial impression of the crack length may be misleading. A comprehensive insight including crack length and load level is required to decide on the brittleness level of the geopolymer concrete. Therefore, the fracture toughness values (K_{IC}^{un}) of the geopolymers were counted up by using the following equation (Tada et al., 2000).

$$K_{IC}^{un} = \frac{1.5PS\sqrt{\pi\alpha}}{bh^{1.5}} f(\alpha) \quad (2)$$

Where P and S indicate the ultimate load and the clear span between the supports. α is the normalized crack length, namely α= a/h. The geometric function *f*(α) is dependent on the span-to-depth ratio and adopted from the study (Ferreira, 2007) for the span-to-depth ratio of 3.

$$f(\alpha) = 60.398928\alpha^5 - 86.787007\alpha^4 + 47.418483\alpha^3 - 8.234774\alpha^2 + 0.092058\alpha + 0.998367 \quad (3)$$

Figure 9 compares the fracture toughness of the geopolymers with different fiber ratios. From the figure, the fracture toughness of the plain geopolymers was 12.8 MPamm$^{0.5}$, which was the lowest value of the fracture toughness of the tested specimens. That finding suggested that the plain specimens had a remarkably brittle characteristic. As for the fiber-reinforced geopolymers, unstable fracture toughness slightly ascended between the G0.6S0 and G0.2S0.4 specimens. However, for the G0S0.6 specimens, unstable fracture toughness decreased abruptly by about 10%. A similar trend was also observed for the standard deviations in the unstable fracture toughness. The main reason for that reduction may be the uneven distribution of the recycled steel fibers at the highest dosages of 0.6 vol%. Compared to industrial steel fibers, recycled steel fibers have an irregular shape, which makes them prone to agglomerate in the mixture. This condition was also pointed out in the literature (Eskandarinia et al., 2022). On the other hand, broadly speaking, the overall average curve may be simplified as a bilinear relation which is composed of a toughness for plain and fiber-reinforced geopolymers. Hence the plateau of the bilinear relation might be defined as 214.2 MPamm$^{0.5}$. This means that the fracture resistance capability of the blend fiber-reinforced geopolymers was almost identical. The possible explanation for the occurrence of that plateau is the inverse relation between the peak load in Figure 7 and the crack length in Figure 8. As the amount of the recycled steel fiber in the hybrid form was raised, the measured peak load decreased, while the average crack length increased. Therefore, the unstable fracture toughness defined as in Equation (2) was slightly changed for the hybrid fibered specimens.

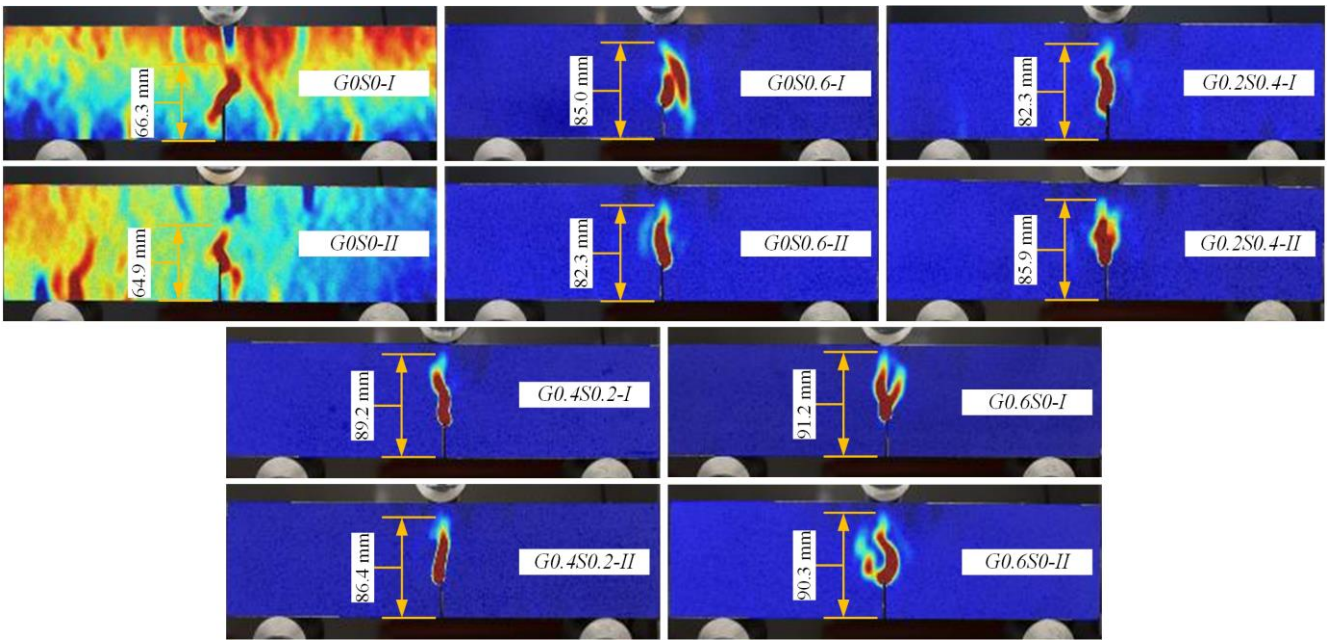

Figure 8. Experimental Crack Length at The Time Of The Peak Load

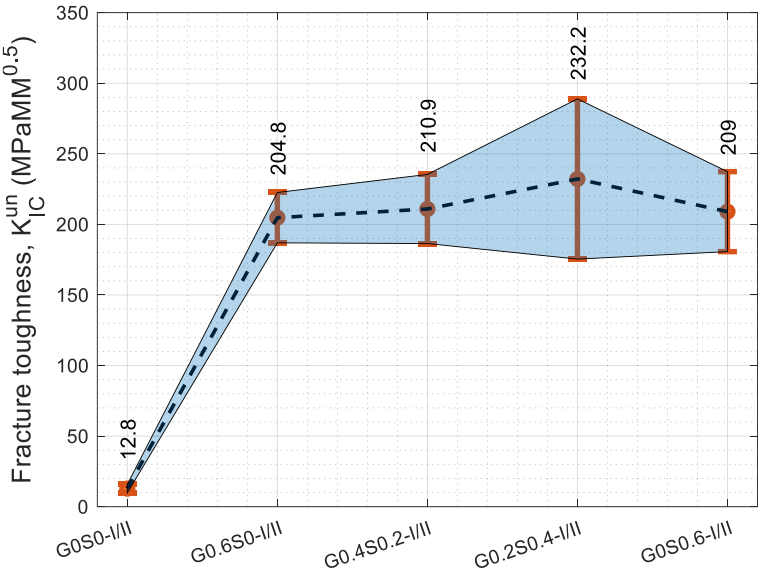

Figure 9. Unstable Fracture Toughness Versus Fiber Content Curve

CONCLUSIONS

In this work, a total of 10 notched beams were tested under a three-point bending test configuration. The deformation loading was applied to the specimens to obtain the post-peak response of the specimens. 5 different mixtures were used such that they contain the plain and hybrid fiber blend at different ratios, meanwhile sum of the fiber dosages was set constant as 0.6 vol%. The measurement of the deformations and strains was taken from the surface of the images through the digital image correlation method. The objective of the experimental study was to examine the effect of the hybridization of glass and recycled steel fibers from the waste tires on the fracture response of the geopolymer concretes. The findings were discussed in terms of load-CMOD curves, crack progress, fracture energy, ultimate load, and unstable fracture toughness. It is worth noting that, unfortunately, the number of specimens used in this work was scarce due to some of the economic concerns and the facilities of the laboratory. Therefore, one should avoid a precise match between the results from this work and the literature. The prominent findings from the present study may be summered in bullet points as follows:

- As the recycled steel fibers were increased from 0 to 0.6% by volume, the measured residual strength at about 4 mm CMODs was gradually decreased from 3.2 kN to 0.77 kN, which corresponded to a drop of about 75.9%. Hence, it may be inferred that the recycled steel fibers were less effective in maintaining the residual strength compared to the glass fibers.
- Compared to the plain matrix, the increase in the initial cracking load was obtained as 607% and 443% for G0.6S0-I and G0S0.6-I specimens, respectively. Therefore, results have shown that glass fibers are a significantly more efficient additive than recycled steel fibers.
- When the volume of recycled steel fibers increased from 0% to 0.6%, the average fracture energy reduced from 2.99 N/mm to 1.14 N/mm due to both the uneven distribution of the steel fibers and the low bonding between steel fibers and concrete.
- The average ultimate load of the fiber-reinforced specimens (G0S0.6) was at least 2.7-fold that of the plain specimens. Also, the ultimate bending load was obtained as 5.27 kN for both the specimens of G0.6S0 and G0.4S0.2.
- The minimum mean crack length measured on the specimens' surface was 65.6 mm for the plain specimens. The mean crack length of the fiber specimen steadily ascended from 83.7 mm to 90.8 mm as the ratio of the recycled steel fibers was changed from 0 to 0.6% in the hybrid blend.
- Compared to the fiber-reinforced specimens, the plain specimens had the lowest fracture toughness value of 12.8 MPamm$^{0.5}$. The low unstable fracture toughness of plain matrix proved their brittle cracking characteristics. On the other hand, the unstable fracture toughness of fiber-reinforced specimens increased at least 15-fold for the G0.6S0 specimen.

REFERENCES

Aisheh, Y.I.A., Atrushi, D.S., Akeed, M.H., Qaidi, S., & Tayeh, B.A. (2022). Influence of steel fibers and microsilica on the mechanical properties of ultra-high-performance geopolymer concrete (UHP-GPC). *Case Studies in Construction Materials*, 17, e01245. https://doi.org/10.1016/j.cscm.2022.e01245

Alsaif, A.S., & Abdulrahman S. Albidah, A. (2022). Compressive and flexural characteristics of geopolymer rubberized concrete reinforced with recycled tires steel fibers. Materials Today: Proceedings, International Conference on Advances in Construction Materials and Structures, 65, (pp. 1230–1236). https://doi.org/10.1016/j.matpr.2022.04.182

Anvari, M., & Toufigh, V. (2022). Experimental and probabilistic investigation on the durability of geopolymer concrete confined with fiber reinforced polymer. *Construction and Building Materials*, 334, 127419. https://doi.org/10.1016/j.conbuildmat.2022.127419

Başaran, B., Aksoylu, C., Özkılıç, Y.O., Karalar, M., & Hakamy, A., (2023). Shear behaviour of reinforced concrete beams utilizing waste marble powder. *Structures*, 54, 1090–1100. https://doi.org/10.1016/j.istruc.2023.05.093

Blaber, J., Adair, B., & Antoniou, A. (2015). Ncorr: Open-Source 2D Digital Image Correlation Matlab Software. *Experimental Mechanics*, 55, 1105–1122. https://doi.org/10.1007/s11340-015-0009-1

Çelik, A.İ., Tunç, U., Bahrami, A., Karalar, M., Othuman Mydin, M.A., Alomayri, T., & Özkılıç, Y.O., (2023). Use of waste glass powder toward more sustainable geopolymer concrete. *Journal of Materials Research and Technology*, 24, 8533–8546. https://doi.org/10.1016/j.jmrt.2023.05.094

da Silva, A.C.R., Almeida, B.M., Lucas, M.M., Cândido, V.S., da Cruz, K.S.P., Oliveira, M.S., de Azevedo, A.R.G., & Monteiro, S.N. (2022). Fatigue behavior of steel fiber reinforced geopolymer concrete. *Case Studies in Construction Materials*, 16, e00829. https://doi.org/10.1016/j.cscm.2021.e00829

Davidovits, J. (1991). Geopolymers. *Journal of Thermal Analysis*, 37, 1633–1656. https://doi.org/10.1007/BF01912193

Ding, Y., Dai, J.-G., & Shi, C.-J. (2016). Mechanical properties of alkali-activated concrete: A state-of-the-art review. *Construction and Building Materials*, 127, 68–79. https://doi.org/10.1016/j.conbuildmat.2016.09.121

Eskandarinia, M., Esmailzade, M., Hojatkashani, A., Rahmani, A., & Jahandari, S. (2022). Optimized Alkali-Activated Slag-Based Concrete Reinforced with Recycled Tire Steel Fiber. *Materials*, 15, 6623. https://doi.org/10.3390/ma15196623

Farhan, N.A., Sheikh, M.N., & Hadi, M.N.S. (2018). Experimental Investigation on the Effect of Corrosion on the Bond Between Reinforcing Steel Bars and Fibre Reinforced Geopolymer Concrete. *Structures*, 14, 251–261. https://doi.org/10.1016/j.istruc.2018.03.013

Ferreira, L.E.T. (2007). Fracture analysis of a high-strength concrete and a high-strength steel-fiber-reinforced concrete. *Mechanics of Composite Materials*, 43, 479–486. https://doi.org/10.1007/s11029-007-0045-8

Ganesh, A.C., & Muthukannan, M. (2021). Development of high performance sustainable optimized fiber reinforced geopolymer concrete and prediction of compressive strength. *Journal of Cleaner Production*, 282, 124543. https://doi.org/10.1016/j.jclepro.2020.124543

Gümüş, M., & Arslan, A. (2019). Effect of fiber type and content on the flexural behavior of high strength concrete beams with low reinforcement ratios. *Structures*, 20, 1–10. https://doi.org/10.1016/j.istruc.2019.02.018

Isa, M.N., Pilakoutas, K., Guadagnini, M., & Angelakopoulos, H. (2020). Mechanical performance of affordable and eco-efficient ultra-high performance concrete (UHPC) containing recycled tyre steel fibres. *Construction and Building Materials*, 255, 119272. https://doi.org/10.1016/j.conbuildmat.2020.119272

Jenq, Y., & Shah, S.P. (1985). Two Parameter Fracture Model for Concrete. *Journal of Engineering Mechanics*, 111, 1227–1241. https://doi.org/10.1061/(ASCE)0733-9399(1985)111:10(1227)

Khan, K., Ahmad, W., Amin, M.N., & Nazar, S. (2022). A Scientometric-Analysis-Based Review of the Research Development on Geopolymers. *Polymers*, 14, 3676. https://doi.org/10.3390/polym14173676

Kumar, Y.N., Dean Kumar, B., & Swami, B.L.P. (2022). Mechanical properties of geopolymer concrete reinforced with steel and glass fibers with various mineral admixtures. Materials Today: Proceedings, International Conference

on Smart and Sustainable Developments in Materials, Manufacturing and Energy Engineering, 52, (pp. 632–641). https://doi.org/10.1016/j.matpr.2021.10.050

Laxmi, G., & Patil, S.G. (2022). Effect of fiber types, shape, aspect ratio and volume fraction on properties of geopolymer concrete – A review. Materials Today: Proceedings, International Conference on Advances in Construction Materials and Structures, 65, (pp. 1086–1094). https://doi.org/10.1016/j.matpr.2022.04.157

Li, W., Shumuye, E.D., Shiying, T., Wang, Z., & Zerfu, K. (2022). Eco-friendly fibre reinforced geopolymer concrete: A critical review on the microstructure and long-term durability properties. *Case Studies in Construction Materials*, 16, e00894. https://doi.org/10.1016/j.cscm.2022.e00894

Mastali, M., Dalvand, A., Sattarifard, A.R., & Illikainen, M. (2018). Development of eco-efficient and cost-effective reinforced self-consolidation concretes with hybrid industrial/recycled steel fibers. *Construction and Building Materials*, 166, 214–226. https://doi.org/10.1016/j.conbuildmat.2018.01.147

Meskhi, B., Beskopylny, A.N., Stel'makh, S.A., Shcherban', E.M., Mailyan, L.R., Shilov, A.A., El'shaeva, D., Shilova, K., Karalar, M., Aksoylu, C., & Özkılıç, Y.O., (2023). Analytical Review of Geopolymer Concrete: Retrospective and Current Issues. *Materials*, 16, 3792. https://doi.org/10.3390/ma16103792

Özkılıç, Y.O., Çelik, A.İ., Tunç, U., Karalar, M., Deifalla, A., Alomayri, T., & Althoey, F., (2023). The use of crushed recycled glass for alkali activated fly ash based geopolymer concrete and prediction of its capacity. *Journal of Materials Research and Technology*, 24, 8267–8281. https://doi.org/10.1016/j.jmrt.2023.05.079

Pająk, M., & Ponikiewski, T. (2013). Flexural behavior of self-compacting concrete reinforced with different types of steel fibers. *Construction and Building Materials*, 47, 397–408. https://doi.org/10.1016/j.conbuildmat.2013.05.072

Qin, X., & Kaewunruen, S. (2022). Environment-friendly recycled steel fibre reinforced concrete. *Construction and Building Materials*, 327, 126967. https://doi.org/10.1016/j.conbuildmat.2022.126967

Ranjbar, N., & Zhang, M. (2020). Fiber-reinforced geopolymer composites: A review. *Cement and Concrete Composites*, 107, 103498. https://doi.org/10.1016/j.cemconcomp.2019.103498

Rashad, A.M. (2020). Effect of steel fibers on geopolymer properties – The best synopsis for civil engineer. *Construction and Building Materials*, 246, 118534. https://doi.org/10.1016/j.conbuildmat.2020.118534

Rashedi, A., Marzouki, R., Raza, A., Ali, K., Olaiya, N.G., & Kalimuthu, M. (2022). Glass FRP-Reinforced Geopolymer Based Columns Comprising Hybrid Fibres: Testing and FEA Modelling. *Polymers*, 14, 324. https://doi.org/10.3390/polym14020324

Ren, R., & Li, L. (2022). Impact of polyethylene fiber reinforcing index on the flexural toughness of geopolymer mortar. *Journal of Building Engineering*, 57, 104943. https://doi.org/10.1016/j.jobe.2022.104943

RILEM-Draft-Recommendation. (1985). Determination of the fracture energy of mortar and concrete by means of three-point bend tests on notched beames. *Materials and Structures*, 18(106), 285-290.

Sherwani, A.F.H., Younis, K.H., & Arndt, R.W. (2022). Fresh, Mechanical, and Durability Behavior of Fly Ash-Based Self Compacted Geopolymer Concrete: Effect of Slag Content and Various Curing Conditions. *Polymers*, 14, 3209. https://doi.org/10.3390/polym14153209

Simalti, A., & Singh, A.P. (2021). Comparative study on performance of manufactured steel fiber and shredded tire recycled steel fiber reinforced self-consolidating concrete. *Construction and Building Materials*, 266, 121102. https://doi.org/10.1016/j.conbuildmat.2020.121102

Tada, H., Paris, P.C., & Irwin, G.R. (2000). The Stress Analysis of Cracks Handbook. (3rd ed.). ASME Press. https://doi.org/10.1115/1.801535

Vijaya Prasad, B., Anand, N., Kiran, T., Jayakumar, G., Sohliya, A., & Ebenezer, S. (2022). Influence of fibers on fresh properties and compressive strength of geo-polymer concrete. Materials Today: Proceedings, International Conference on Innovation and Application in Science and Technology, 57, (pp. 2355–2363). https://doi.org/10.1016/j.matpr.2022.01.426

Wang, T., Fan, X., Gao, C., Qu, C., Liu, J., & Yu, G. (2023). The Influence of Fiber on the Mechanical Properties of Geopolymer Concrete: A Review. *Polymers*, 15, 827. https://doi.org/10.3390/polym15040827

Wang, Yi., Chan, C.L., Leong, S.H., & Zhang, M. (2020). Engineering properties of strain hardening geopolymer composites with hybrid polyvinyl alcohol and recycled steel fibres. *Construction and Building Materials*, 261, 120585. https://doi.org/10.1016/j.conbuildmat.2020.120585

Wang, Yijiang., Zheng, T., Zheng, X., Liu, Y., Darkwa, J., & Zhou, G. (2020). Thermo-mechanical and moisture absorption properties of fly ash-based lightweight geopolymer concrete reinforced by polypropylene fibers. *Construction and Building Materials*, 251, 118960. https://doi.org/10.1016/j.conbuildmat.2020.118960

Wang, Z., Bai, E., Huang, H., Liu, C., & Wang, T. (2023). Dynamic mechanical properties of carbon fiber reinforced geopolymer concrete at different ages. *Ceramics International*, 49, 834–846. https://doi.org/10.1016/j.ceramint.2022.09.056

Yolcu, A., Karakoç, M.B., Ekinci, E., Özcan, A., & Sağır, M.A. (2022). Effect of binder dosage and the use of waste rubber fiber on the mechanical and durability performance of geopolymer concrete. *Journal Building Engineering*, 61, 105162. https://doi.org/10.1016/j.jobe.2022.105162

Zada Farhan, K., Azmi Megat Johari, M., & Demirboğa, R. (2022). Evaluation of properties of steel fiber reinforced GGBFS-based geopolymer composites in aggressive environments. *Construction and Building Materials*, 345, 128339. https://doi.org/10.1016/j.conbuildmat.2022.128339

Zhong, H., Poon, E.W., Chen, K., & Zhang, M. (2019). Engineering properties of crumb rubber alkali-activated mortar reinforced with recycled steel fibres. *Journal of Cleaner Production*, 238, 117950. https://doi.org/10.1016/j.jclepro.2019.117950